Two interacting particles in a disordered chain III: Dynamical aspects of the interplay disorder-interaction

S. De Toro Arias[1,2], X. Waintal[1], and J.-L. Pichard[1,a]

[1] CEA, Service de Physique de l'État Condensé, Centre d'Études de Saclay, 91191 Gif-sur-Yvette Cedex, France
[2] Laboratoire de Physique de la Matière Condensée[b], Université de Nice-Sophia Antipolis, Parc Valrose, BP 71, 06108 Nice Cedex 2, France

Abstract. The interplay between the quantum interferences responsible for one particle localization over a length L_1, and the partial dephasing induced by a local interaction of strength U with another particle leading to partial delocalization over a length $L_2 > L_1$, is illustrated by a study of the motion of two particles put close to each other at the initial time. Localization is reached in two steps. First, before the time t_1 necessary to propagate over L_1, the interaction slows down the ballistic motion. On the contrary, after t_1 the interaction favors a very slow delocalization, characterized by a $\log(t)$ spreading of the center of mass, until L_2 is reached. This slow motion is related to the absence of quantum chaos in this one dimensional model, the interaction being only able to induce weaker chaos with critical spectral statistics. Under appropriate initial conditions, the motion remains invariant under the duality transformation mapping the behavior at small U onto the behavior at large U.

PACS. 71.10.-w Theories and models of many electron systems – 71.30.+h Metal-insulator transitions and other electronic transitions – 73.20.Jc Delocalization processes

1 Introduction

In this third work of a series [1–3] concerning two interacting particles (TIP) in a one dimensional random lattice, we use the time dependent Schrödinger equation to describe the competition between the one particle quantum interferences induced by the random potential leading to localization, and the mutual dephasing induced by a local interaction and leading to partial delocalization. At the initial time, a wave packet representing two particles in two neighboring sites is constructed in the middle of a disordered chain of size L. A repulsive on site interaction of strength U is considered. The particles are assumed to be two electrons with opposite spins, the initial wave function is symmetric and remains symmetric during the quantum motion. We study the short times where the particles visit scales small compared to the one particle localization length L_1 till the long times where the spreading of the center of mass saturates at the TIP localization length $L_2 \gg L_1$. For this, we use an efficient automaton-like algorithm adapted to discrete scalar wave propagation in a system of finite size L. We restrict the study to strong localization, such that the quantum motion is the same when the size increases from $L = 512$ to $L = 1024$ and $t \to \infty$. This guarantees that our con-

clusions are not biased by finite size effects coming from successive boundary reflexions. The price to pay for this is to consider relatively small values for L_1 and L_2.

The TIP-dynamics is characterized by two times t_1 and t_2, where a scale of order of L_1 and L_2 is respectively explored. Between t_1 and t_2, we find that the spreading of the center of mass is extremely slow. To give an order of magnitude, $L_1 \approx 16$ can be quickly reached after $t_1 \approx 100$ (in units of time) while a time $t_2 \approx 10^4$ is necessary to reach only $L_2 \approx 2L_1$. In this regime of interaction assisted propagation, we find that the center of mass spreads with a $\log(t)$-law, quite different from a previously assumed diffusion law. This is consistent with the observation [2] that the interaction can never drive the TIP system in one dimension to full quantum chaos with Wigner-Dyson spectral statistics. Only a weak critical chaos can be established, where the spectral fluctuations are statistically similar to those characterizing [4] different critical one particle spectra ($3d$ Anderson model at the mobility edge [5] or certain pseudo-integrable billiards). Another important phenomenon illustrated by this study is the inversion of the effect of the interaction when the ballistic motion ($t < t_1$) becomes sub-diffusive ($t_1 < t < t_2$): first U defavors the ballistic propagation before having an opposite delocalizing effect.

The paper is organized as follows. The model and the used algorithm are introduced (Sect. 2). Then a series

of useful results for understanding the complex features of TIP dynamics (Sect. 3) are shortly summarized. Illustrations of the TIP delocalization phenomenon are given when $t \to \infty$. The role of the finite size effects are studied for $L = 512$, and the values of L_1 and L_2 where they can be neglected are estimated (Sect. 4). In the remaining part, we study how is reached this long time limit, after two successive regimes of the quantum motion. First, a ballistic regime ($t < t_1$) is studied where U defavors propagation (Sect. 5). The dependence of the TIP dynamics on the chosen initial wave packet is illustrated. We consider both two particles put at $t = 0$ on the same site (energy $\approx U$) and on two neighboring sites (energy ≈ 0). Following the initial condition, the dynamics probes two different sets of states in the large U-limit: molecular states of energy $\approx U$ and hard core boson states of energy ≈ 0, as discussed in reference [2]. The duality transformation mapping the behavior at small U onto the behavior at large U is illustrated for appropriate initial conditions. A study of t_1 follows (Sect. 6) before describing the sub-diffusive regime where interaction favors a slow TIP propagation ($t_1 < t < t_2$: Sect. 7). The $\log(t)$ spreading of the center of mass is related to the long life-time observed in reference [1] for the free boson states (TIP states for $U = 0$). The relation between the observed very slow delocalization, the multifractal measure [1] characterizing the interaction induced hopping terms coupling the free boson states, and the critical weak chaos observed in reference [2] are discussed.

2 Model and numerical algorithm

To study the motion of two electrons with opposite spins in a one dimensional Anderson tight binding model with on site interaction, we have to numerically solve the discretized TIP Schrödinger equation:

$$\frac{\mathrm{i}}{2\epsilon}\left(|\psi(t+\epsilon)\rangle - |\psi(t-\epsilon)\rangle\right) = \mathcal{H}|\psi(t)\rangle, \qquad (1)$$

where $\mathcal{H} = H_0 \otimes 1 + 1 \otimes H_0 + H_{\mathrm{int}}$. H_0 is the one particle tight binding Anderson Hamiltonian:

$$H_0 = \sum_{n=1}^{L-1}\left(|n\rangle\langle n+1| + |n+1\rangle\langle n|\right) + \sum_{n=1}^{L} V_n |n\rangle\langle n|.$$

L is the system size and V_n are independent random variables, uniformly distributed inside the interval $[-W, W]$. The ket $|n\rangle$ stands for the electronic orbital located at the site n of the one dimensional lattice. The eigenstates $|\alpha\rangle$ of H_0 are localized on a length L_1 (with $L_1 \approx 24/W^2$ at the band center). H_{int} is the on site interaction:

$$H_{\mathrm{int}} = U \sum_{n=1}^{L} |n\rangle \otimes |n\rangle\langle n| \otimes \langle n|.$$

In what follows, all the lengths are given in lattice spacing units and all the energies in units of $1/\epsilon$. The times are

then expressed in the corresponding units (ϵ). The sites are labelled from $-L/2$ to $+L/2$, such that the site $n = 0$ is located in the middle of the chain. The initial condition corresponds to

$$\psi_{n_1,n_2}(0) = \psi_{n_1,n_2}(\epsilon) = \frac{1}{\sqrt{2}}(\delta_{n_1,0}\delta_{n_2,\rho_0} + \delta_{n_2,0}\delta_{n_1,\rho_0}),$$

where $\langle n_1 n_2 | \psi(t)\rangle = \psi_{n_1,n_2}(t)$.

When ϵ is small enough, the discrete time equation (1) has the same physical content as its continuous version.

To solve equation (1), we use an automaton-like algorithm [6], which relies on a formulation of discrete scalar wave propagation in an arbitrary inhomogeneous medium by the use of elementary processes obeying a discrete Huygens' principle and satisfying fundamental symmetries, as described in reference [6]. Our algorithm avoids the direct discretisation procedure and incorporates the symmetries underlying the Anderson model at the lowest stage of the construction. As a consequence the algorithm preserves the unitarity of the dynamics, insuring the normalization of the wavefunction at all times, $\sum_{n_1,n_2} |\psi_{n_1,n_2}(t)|^2 = 1$, up to a small correction of order ϵ^2. Besides, the construction is optimized for implementing the algorithm on massively parallel machines. The numerical simulations have been carried for a time step $\epsilon = 0.05$. The simulations were performed on a 16K processor Connexion Machine. Given a value of the disorder strength W and a disorder configuration, the wavefunction has been calculated for chains of length as large as $L = 1024$ and up to a maximum of 10^6 units of time.

3 Review of some useful results

Since the two body quantum motion is quite complex, it is useful to have in mind a few previous results that we shortly summarize.

3.1 Non linear σ model

The first analytical descriptions [7,8] of the TIP system are mainly based on simplified random matrix Hamiltonians with independent Gaussian entries. The purpose was first to explain the new phenomenon of pair propagation at scales larger than L_1 and the pair localization at a scale $L_2 \gg L_1$. In reference [8], from such an effective random matrix Hamiltonian, a supersymmetric nonlinear σ model was derived, closely related with the one found by Efetov for non interacting electrons in disordered metals. The approach was mainly developed for an arbitrary dimension d. We recall the conclusions for a strictly one dimensional model ($d = 1$).

Let us denote by $|\alpha\rangle$ a one particle state located near the site n_α, $|\alpha\beta\rangle$ the symmetrized product states forming the eigenbasis of the TIP Hamiltonian when $U = 0$. Since they are the symmetric eigenstates without interaction, we call them "free boson states" as in references [2,3].

We denote by $\Gamma_{\alpha\beta}$ their inverse lifetime when the interaction is switched on. The TIP supersymmetric σ model gives $\Gamma_{\alpha\beta}$ in agreement with the Fermi golden rule:

$$\Gamma_{\alpha\beta} \sim 2\pi |\langle\alpha\beta|H_{\mathrm{int}}|\alpha\beta\rangle|^2 \nu_{\mathrm{eff}} \approx \Gamma_1 f\left(\frac{|n_\alpha - n_\beta|}{L_1}\right), \quad (2)$$

where

$$\Gamma_1 \approx 2\pi \frac{U^2}{BL_1}. \qquad (3)$$

B is the kinetic energy (band width), $\langle\alpha\beta|H_{\mathrm{int}}|\gamma\delta\rangle$ the typical interaction matrix element between two free boson states and ν_{eff} the density of free boson states $|\gamma\delta\rangle$ coupled to $|\alpha\beta\rangle$ by the interaction. $f(x) \approx 1$ when $x < 1$, *i.e.* when the typical distance $|n_\alpha - n_\beta|$ between the localized states $|\alpha\rangle$ and $|\beta\rangle$ is smaller than L_1 and $f(x) \approx \exp(-x)$ when $|n_\alpha - n_\beta| > L_1$. The lifetime of $|\alpha\beta\rangle$ depends on the spatial overlap between $|\alpha\rangle$ and $|\beta\rangle$. Localized at a distance $|n_\alpha - n_\beta|$ large compared to L_1, the two particles have an exponentially small probability to be on the same site and to feel the on site interaction. The corresponding lifetime is exponentially large. For $|\alpha\rangle$ and $|\beta\rangle$ localized inside the same localization domain of size L_1, the lifetime Γ_1^{-1} defines an important characteristic time. In reference [8], Γ_1^{-1} and L_1 are respectively the smallest resolved time and length scales. The main assumption of the approach, contained in the effective random matrix Hamiltonian from which the σ model is derived, is that the one particle states are essentially ergodic, chaotic and random inside their localization domain. This is a simplification of the one body dynamics inside L_1, which amounts to assume for the single particle a "zero-dimensional" dynamics inside L_1. For $L = L_1$, one gets $\langle\alpha\beta|H_{\mathrm{int}}|\gamma\delta\rangle \approx \pm U/L_1^{3/2}$ and $\nu_{\mathrm{eff}} \approx L_1^2/B$ near the band center, and eventually the above expression for Γ_1. As far as the dynamics are concerned, the main conclusions of reference [8] are as follows. For $t > \Gamma_1^{-1}$, the time where the pair size $\rho(t)$ is roughly equal to $|n_\alpha - n_\beta|$ can be estimated from the lifetime of the free boson state $|\alpha\beta\rangle$ with $|n_\alpha - n_\beta| \approx \rho(t)$. This gives

$$\rho(t) \propto L_1(1 + \log(\Gamma_1 t)). \qquad (4)$$

At the same time, the center of mass $R(t)$ exhibit a diffusive motion $R(t) = \sqrt{D_2(t)t}$, with a slightly time dependent diffusion constant $D_2(t) \approx (U^2/B)(L_1/\log(\Gamma_1 t))$. This small time dependence of $D_2(t)$ comes from the fact that the frequency of the collisions between the two particles decreases as the pair size grows. This diffusion stops when $R(t) \approx L_2 \approx (U/B)^2 L_1^2$, where TIP localization occurs.

3.2 Level curvature

Useful, though indirect information for the TIP propagation at scales $L \leq L_1$ can be found in reference [9] where the sensitivity of the TIP levels E_A to a change of boundary conditions is given. Detailed numerical calculations confirming the predictions of reference [9] are given in the last paper of this series [3]. For a ring threaded by an AB-flux Φ, the TIP curvature $C_2(E) \equiv \sum_A \frac{\partial^2 E_A}{\partial \Phi^2} \delta(E - E_A)$ is given by the expression:

$$C_2(E) \approx g_1 \frac{\Delta_1}{\Delta_2} - (g_1 - 1) g_2(U) \frac{\Delta_1}{B}. \qquad (5)$$

g_1 and Δ_1 are respectively the one particle conductance and mean level spacing. $g_2(L, U)$ can be understood as an interaction-assisted TIP conductance [10] of order $\Gamma_{\alpha\beta}(L, U)/\Delta_2(L)$, where $\Delta_2(L)$ is the spacing of the free boson levels directly coupled by the interaction. The above expression implies that the effect of U strongly depends on L. When $L \ll L_1$, $g_1 - 1 \approx g_1$, and C_2 is mainly given by a kinetic one particle term $g_1 \Delta_1/\Delta_2$ *reduced* by a small correction proportional to $g_2(L, U)$. This means that for $L \ll L_1$ (ballistic one particle regime) the easy propagation due to kinetic terms is not yet strongly affected by the one particle quantum interference. In this case, the presence of the second particle defavors the propagation of the first and the interaction slightly reduces C_2, as confirmed in reference [3]. When $L \geq L_1$, the one particle transport is suppressed by the quantum interferences (Anderson localization) and the term proportional to U in C_2 *changes its sign*, since $g_1 - 1 \approx -1$ up to exponentially small corrections. Thus, TIP transport is *favored* by the interaction, the presence of the second particle leading to a decoherence of the localizing quantum interferences of the first. C_2 is of order g_2 for the few TIP states reorganized by the interaction when $L \gg L_1$. From the behavior of the TIP curvature, one should expect a change of the role of U for the TIP quantum motion as a function of time: starting from a localized wave packet, the exploration on a scale $L \leq L_1$ for $t < t_1$ should require a *longer* time with interaction than without. But without interaction, the exploration of scales $L \gg L_1$ is forbidden by Anderson localization, while it becomes possible in the presence of interaction. An important issue is then to know what is the time scale $t_2 - t_1$ required for this exploration, before the pair itself gets localized when $t \approx t_2$. According to reference [8], $t_2 - t_1 = \sqrt{L_2/D_2(t_2 - t_1)}$. However, one should have in mind some further results obtained for strictly on site interaction and strictly one dimension.

3.3 Multifractality

The interaction matrix elements

$$\langle\alpha\beta|H_{\mathrm{int}}|\gamma\delta\rangle = 2U \sum_{n=1}^{L} \Psi_\alpha^*(n)\Psi_\beta^*(n)\Psi_\gamma(n)\Psi_\delta(n),$$

(with $\Psi_\alpha(n) = \langle n|\alpha\rangle$) defines a measure of the free boson states $|\gamma\delta\rangle$ coupled to a given $|\alpha\beta\rangle$. It was shown in reference [1] that this measure is multifractal. In contrast to earlier assumptions, the density $\nu_{\mathrm{eff}}(L)$ of free boson states $|\gamma\delta\rangle$ effectively coupled to $|\alpha\beta\rangle$ is much weaker than the total density $\nu_2(L)$ of free boson states. This is

not surprizing when there is no disorder: only free boson states of same total momentum are directly coupled, and $\nu_{\text{eff}} = \nu_1 \propto L$ and not $\nu_2 \propto L^2$. When disorder is switched on, the momentum is no longer a good quantum number, and one gets $\nu_1 < \nu_{\text{eff}} < \nu_2$. More precisely, if one wants to estimate $\Gamma_{\alpha\beta}$ using the Fermi golden rule, one needs the *effective* density of states $|\gamma\delta\rangle$ coupled by the second moment $(q = 2)$ of the interaction matrix elements. The measure in the TIP Hilbert space of the support of this set of states is neither $d = 1$ (as for the clean case) nor $d = 2$ (as for the chaotic $d = 0$ case), but a fractal dimension $1 < f(\alpha(q = 2)) \approx 1.75 < 2$. This gives a reduced effective density $\nu_{\text{eff}} \propto L^{f(\alpha(q=2))}$. The measure is multifractal, since this density depends on the considered qth moment of the coupling term. A direct implication of this multifractal character is that the lifetime of the free boson states is longer than Γ_1 for $L \approx L_1$. One should expect that the diffusion law obtained ignoring multifractality underestimates the time $t_2 - t_1$ for the particles to propagate between L_1 and L_2. The multifractality of the set of directly coupled free boson states should mean a *very slow* interaction induced delocalization.

3.4 Weak critical chaos

The TIP spectral fluctuations also lead us to expect very slow dynamics before localization. For a given L, the TIP spectrum has Poisson statistics in the limits where either the disorder W or the interaction U are too weak or too strong. In the limit of the clean system $(W = 0)$, this is due to the fact that the effective density of coupled free boson states is $\nu_1 \propto L \ll \nu_2 \propto L^2$. For $W \gg 1$, one has $L_1 \ll L$ and the small part of TIP levels being reorganized by U is totally hidden behind the main part of the non reorganized spectrum, corresponding to free boson states with $|n_\alpha - n_\beta| \geq L_1$ and which remain eigenstates when U is switched. For $U \ll 1$, the TIP states are basically the free boson states of energy $\epsilon_\alpha + \epsilon_\beta$, *i.e.* almost uncorrelated TIP-levels. For $U \gg 1$, the levels have again an energy $\epsilon_\alpha + \epsilon_\beta$ (duality property explained in the next paragraph). In the plane (U, W), inside those mentioned Poisson limits, in a domain centered around $L \approx L_1$ and $U \approx 1$, the TIP spectrum becomes more rigid, though less rigid than a Wigner-Dyson spectrum associated to quantum chaos. The spectral rigidity saturates [2] to an intermediate rigidity between Poisson and Wigner-Dyson. This rigidity is however not arbitrary, but has a *universal* character shared by many one particle "critical" systems [4], such as the Anderson model at the mobility edge, a mixed system where integrable and chaotic trajectories coexist or a pseudo-integrable billiard where all trajectories belong to a surface of genus larger than one. By the term "weak critical chaos", we mean that under certain circumstances ($U \approx 1$ and $L \approx L_1$), the TIP system belongs to the same critical universality class than those one particle systems, at least as far as the spectral statistics are concerned. The interaction can never drive the TIP system towards a stronger chaos, *i.e.*, towards full quantum chaos with Wigner-Dyson statistics.

3.5 Duality

The Hamiltonian without interaction is diagonal in the basis of the free boson states. As pointed out by Ponomarev and Silvestrov [11], there is an eigenbasis appropriate when $U \to \infty$, having the same energies $\epsilon_\alpha + \epsilon_\beta$ than the free boson states. Indeed, when $U \to \infty$, one has just to solve a non interacting problem with new boundary conditions. Since particles cannot be on the same site, we define $L(L - 1)/2$ hard core boson states $|hc\rangle$ of components $\langle n_1 n_2 | hc \rangle$ given by

$$\frac{1}{\sqrt{2}} \left[\Psi_\alpha(n_2)\Psi_\beta(n_1) - \Psi_\alpha(n_1)\Psi_\beta(n_2) \right] \frac{n_2 - n_1}{|n_2 - n_1|}. \qquad (6)$$

A hard core boson state is just a 2×2 antisymmetric Slater determinant resymmetrized by the factor $(n_2 - n_1)/|n_2 - n_1|$. To complete this basis of the symmetric TIP Hilbert space spanned by $L(L + 1)/2$ states, we add L molecular states $|nn\rangle$ of energy $2V_n + U$, V_n being the random potential of the nth site. This set of molecular states forms a small sub-band which goes to very large energies when $U \to \infty$. For the main sub-band of hard core bosons states, centered around $E = 0$ as the free boson states, there is a duality relation [2,11] $U \leftrightarrow A/U$, mapping the behavior at small U onto the behavior at large U. $A = \sqrt{24}$ for $E = 0$. One finds that the coupling terms between the free boson states are given by

$$2U \sum_n \Psi_\alpha^*(n)\Psi_\beta^*(n)\Psi_\gamma(n)\Psi_\delta(n),$$

while the coupling terms between the hard core boson states are a sum of terms like

$$\sum_{n,n',n''} \frac{\Psi_\alpha^*(n)\Psi_\beta^*(n)\Psi_\gamma(n')\Psi_\delta(n'')}{U + 2V_n - E},$$

with various combinations of $n', n'' = n \pm 1$. The duality is obtained neglecting the difference between n and n' and assuming that $U + 2V_n - E \approx U$. This gives a strong dependence of the TIP dynamics on the initial wave packet. For large U, the $(|hc\rangle \cup |nn\rangle)$ form an eigenbasis, the motion of a wave packet located at the sites 0 and ρ_0 for $t = 0$ is given by the time dependent wave function:

$$\psi_{n_1,n_2}(t) = \sum_{S=(hc,nn)} C_{n_1,n_2,S}^* C_{0,\rho_0,S} e^{-iE_S t},$$

where the summation S goes over the states $|hc\rangle$ and $|nn\rangle$ and $C_{n_1,n_2,S} = \langle n_1, n_2 | S \rangle$. For two particles put on the same site n at the beginning (*i.e.* with an energy $U + 2V_n$), we mainly probe the molecular state $|nn\rangle$ when U is large: the two particles stay on the same site for a very large time. For smaller values of U, this initial wave packet starts to probe the molecular state $|nn\rangle$ before decaying onto the neighboring hard core bosons states of energy of order U. To eliminate the time motion associated with the molecular states and to see the time motion associated to the hard core boson states, which only exhibit the duality property, one has to start with two particles put close to each other on two *different* sites 0 and ρ_0.

4 Asymptotic TIP localization and finite size effects

The role of the repulsive interaction U on the quantum motion is shown in Figures 1 and 2, illustrating the TIP delocalization effect [7] in a strongly disordered chain for $U = 1$. This effect is a consequence of the mixing by the interaction of free boson states close in energy, delocalizing the TIP system in the free boson basis. Since the one body states are localized, this delocalization in the free boson basis also means delocalization in real space. The initial condition corresponds to $\rho_0 = 1$. We have taken the site potentials $V_0 = V_1 = 0$, in order to benefit by the large density of TIP states for $E \approx 0$.

In Figures 1 and 2, the rainbow color code indicates on a linear scale the small values of $|\psi_{n_1,n_2}(t = 5 \times 10^4)|^2$ in red up to the large values in violet. In the upper Figure 1, one can see how the two particles are confined by the random potential without interaction, in a localization domain which is very quickly reached (typically for $t \approx 200$). In the lower Figure 1, $U = 1$ and the center of mass becomes delocalized as sketched in the upper Figure 2. TIP localization after ensemble averaging is shown on the lower Figure 2 for $U = 1$. This TIP ellipsoidal localization domain is reached and stops to spread after a considerably larger time (typically for $t \approx 5 \times 10^4$). For a given sample, one can see that $|\psi_{n_1,n_2}(t = 5 \times 10^4)|^2$ does not homogeneously fill the ellipse, and is characterized by large fluctuations, mainly near the border of the ellipse. These fluctuations are somewhat similar to those characterizing the interaction matrix elements coupling the free boson states (see Fig. 1 of Ref. [1]). As we have checked, $\psi_{n_1,n_2}(t)$ develop an anisotropic multifractal behavior when the interaction assisted propagation begins to dominate the dynamics.

To study the spreading $R(t)$ of the center of mass and the size $\rho(t)$ of the pair, we use the following functions:

$$R(t) = \left(\sum_{n_1,n_2} |\psi_{n_1,n_2}(t)|^2 \frac{(n_1 - \bar{n}_1 + n_2 - \bar{n}_2)^2}{2} \right)^{1/2},$$

$$\rho(t) = \left(\sum_{n_1,n_2} |\psi_{n_1,n_2}(t)|^2 \frac{(n_1 - \bar{n}_1 - n_2 + \bar{n}_2)^2}{2} \right)^{1/2},$$

where $\bar{n}_{1,2} = \sum_{n_1,n_2} |\psi_{n_1,n_2}(t)|^2 n_{1,2}$. We have checked that the disorder average of $\bar{n}_{1,2}$ does not depend on time.

Before going further, we first check that the localization effects are strong enough so that the TIP motion that we study corresponds to the dynamics of the infinite chain, and not of a finite chain with boundary effects. Indeed, for a too weak disorder, fast fronts of the wave function could propagate [12] up to the boundaries and be reflected. This will affect the long time behavior, as the reflected waves enhance the localization of the center of mass. The enhancement factor for $R(t)$ would be underestimated. Since our numerical algorithm allows to study systems of size up to $L = 1024$ for 10^6 steps of time, we compare in Figure 3 the motion for $L = 512$ and $L = 1024$ and for $L_1 = 16$ and $L_1 = 36$.
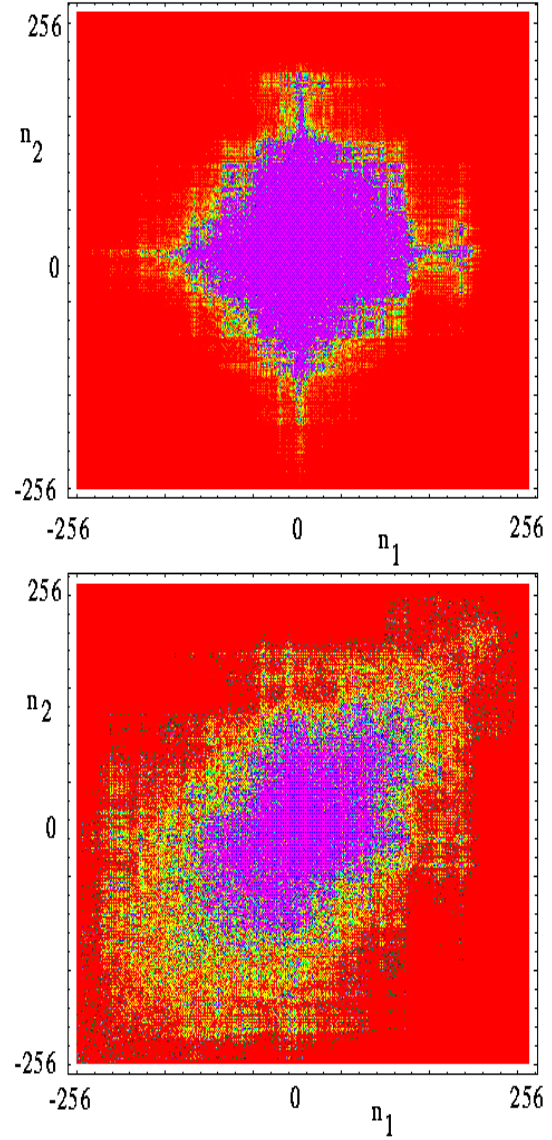

Fig. 1. $|\psi_{n_1,n_2}(t = 5 \times 10^4)|^2$ for two particles put on sites 0 and $\rho_0 = 1$ at $t = 0$. $L = 512$ and $L_1 = 16$. Up: $U = 0$. Down: $U = 1$.

For $L_1 = 16$, $R(t)$ saturates at the same value $L_2 \approx 36$ when the size $L = 512$ is doubled, while $R(t)$ has strong finite size effects for $L_1 = 36$ above $t \approx 10^3$ when $L = 512$. The study of TIP delocalization in the infinite chain can be investigated when $L = 512$ only for a large disorder, where both L_1 and L_2 are relatively small. Since L_2 is reached after a very long time, our numerical method is not convenient to study how L_2 depends on L_1 and U. We just show in Figure 4 the probability density $p(R) \equiv \sum_{n_1+n_2=R} |\psi_{n_1 n_2}(t = 5 \times 10^4)|^2$ for $U = 0$ and $U = 1$ when $L_1 = 16$. This proves that the center of mass is indeed exponentially localized over a length $L_2 \approx 2L_1$, without finite size effect. For larger values of L_1 we have seen larger effects ($R(U = 1)/R(U = 0) \approx 3.5$) at long times, but this only gives a lower estimate for the enhancement factor L_2/L_1, boundary effects being non negligible.
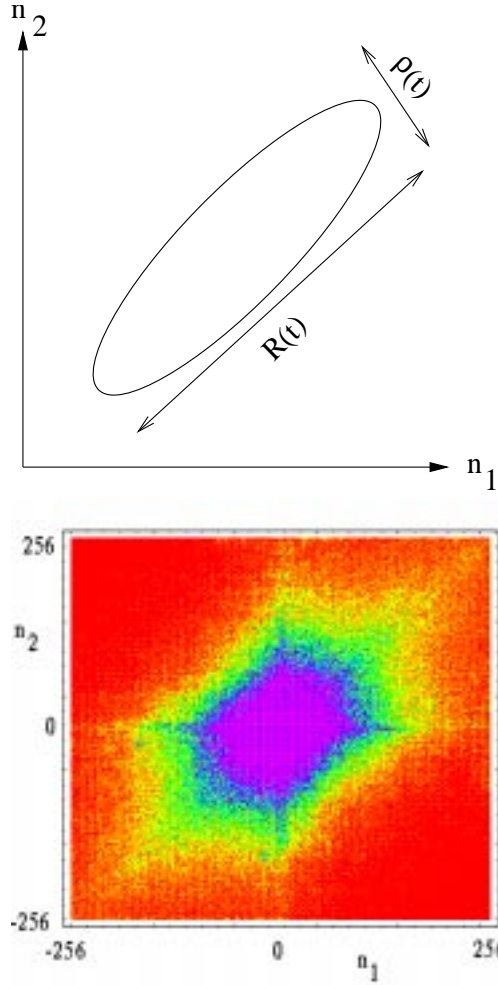
Fig. 2. Up: scheme of the TIP delocalization effect: $|\psi_{n_1,n_2}(\infty)|^2$ is concentrated in an ellipse corresponding to a center of mass R delocalized by the interaction on a scale larger than the pair size ρ. Down: same as in Figure 1 for $U = 1$, $L_1 = 36$ after having averaged over 20 samples.
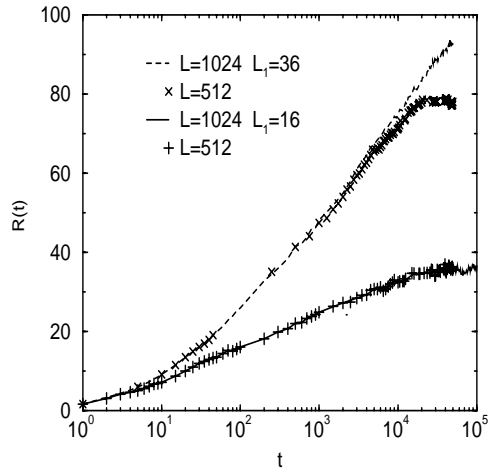

Fig. 3. Finite size effects for $U = 1$. $R(t)$ for $L_1 = 16$ and 36 for two sizes $L = 512$ and 1024.
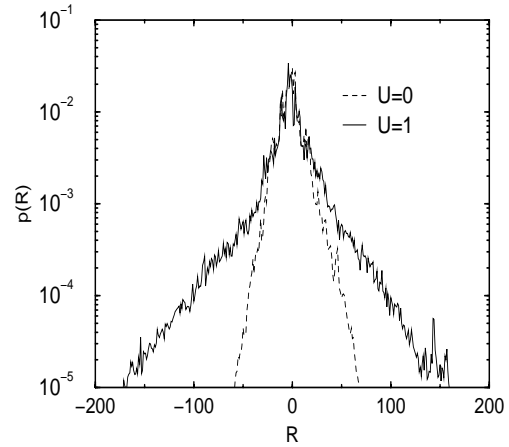

Fig. 4. TIP delocalization effect. Probability distribution $p(R(t = 5 \times 10^4))$ for a single sample with $L_1 = 16$, $L = 1024$, $U = 0$ (dashed line) and $U = 1$ (thick line).

The different regimes of the quantum motion

We now study the intermediary time scales during which the center of mass $R(t)$ spreads, before the time t_2 where it saturates and TIP localization occurs. For $U = 0$, the aspect ratio of $|\psi_{n_1,n_2}(t)|^2$, defined by $R(t)/\rho(t)$, remains equal to one at all times, but for $U \neq 0$, the time evolution of this ratio exhibits three regimes (Fig. 5), delimited by two characteristic time scales t_1 and t_2. For $t \leq t_1$, the repulsive interaction favors $\rho(t)$ and defavors $R(t)$. The ratio $R(t)/\rho(t)$ decreases. This is the ballistic regime characterizing the length scales smaller than L_1. The situation is opposite for $t_1 < t < t_2$ where L_1 has been reached and the interaction assisted propagation of the center of mass begins, on scales larger than L_1. The increase of $R(t)$ is now much faster than the increase of $\rho(t)$, and the ratio $R(t)/\rho(t)$ increases. L_2 is reached at $t = t_2$ where TIP localization occurs.

5 Ballistic propagation and duality

For $t \leq t_1$ we find that the spreading of the center of mass is almost ballistic:

$$R(t) \sim v(U)t^{\mu(U)} \quad \text{with} \quad \mu(U) \approx 1,$$

and that the interaction reduces the increase of $R(t)$. The time evolution strongly depends on the initial condition. When the two particles are injected on the same site at $t = 0$, with an energy of order U, the spreading of the center of mass is almost suppressed by a too large interaction. This is the dynamics associated to the molecular states $|nn\rangle$, which do not decay when U becomes very large (Fig. 6).

On the contrary, injecting the two particles at two neighboring sites ($\rho_0 = 2$), one can see the dynamics associated to the hard core boson states and the consequence of the duality relation $U \leftrightarrow 1/U$ between the free bosons
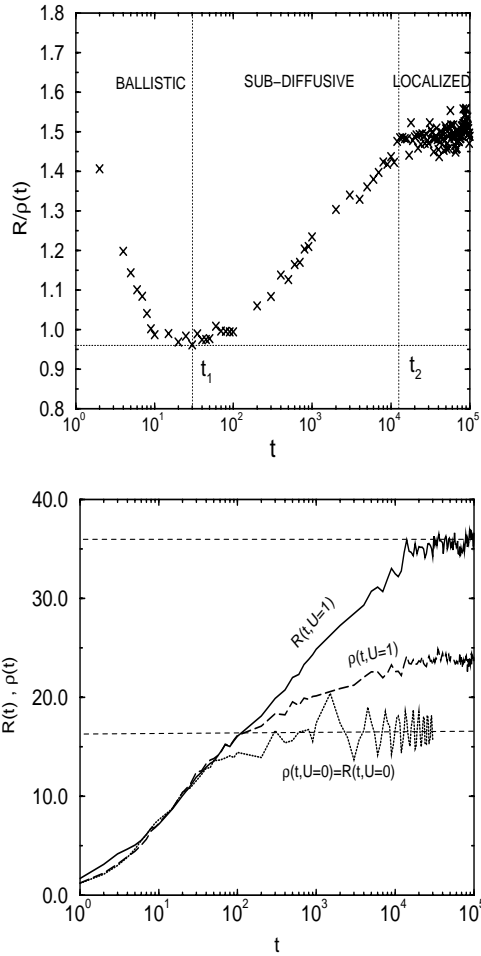
Fig. 5. Single sample with $L_1 = 16, L = 1024$ and $U = 1$. Up: $R(t)/\rho(t)$. Down: $R(t)$, $\rho(t)$ and $\rho(t)$ for $U = 0$ and $U = 1$.
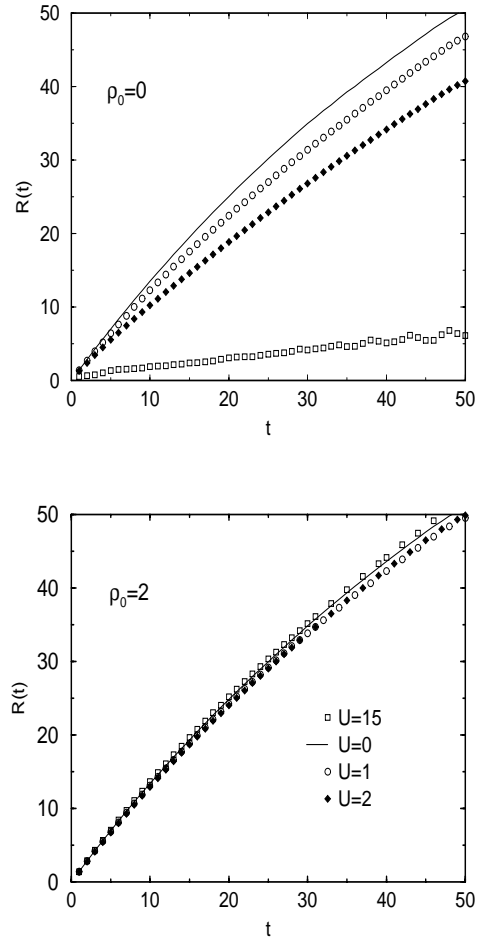
Fig. 6. $R(t)$ at small times for different values of the interaction. $L_1 = L = 200$, average over 20 samples. Up: $\rho_0 = 0$. Down: $\rho_0 = 2$.

and the hard core bosons. Since the density of those states exhibits a Van Hove singularity at $E = 0$ for $U, W = 0$, we have also taken $V_0 = V_{\rho_0} = 0$. This optimizes the coupling between $\psi(t = 0)$ and the hard core spectrum. The duality shows up in the quantum motion. In Figure 6, when $\rho_0 = 2$,

(i)   that $R(t)$ increases almost linearly as a function of t (*i.e.* that the motion is almost ballistic,
(ii) $R(t)$ decreases with U ($U < 2$),
(iii) that $R(t)$ is very similar when $U = 0$ and $U = 15$ (duality).

   In Figure 7, the averages over the random potential of $R(t = 40)$ and $R(t = 1000)$ are shown as a function of the strength U of the interaction. The upper figure corresponds to the ballistic regime where U defavors transport, while the lower figure corresponds to the case where U has started to favor transport. The two curves illustrate the consequences of the duality between the free bosons and the hard core bosons and the inversion of the role of U around t_1.

6 Scaling in the ballistic regime

To define the characteristic time t_1 separating the ballistic and sub-diffusive regimes, one can use many criteria. For instance, t_1 can be defined

(i)   as the lifetime $\hbar/\Gamma_1$ of the free (hard core) boson states, when $U < U_c \approx 2$ ($U > U_c$);
(ii) as the time t_1^R where the particles reach the one particle localisation length L_1 when $R(U, t_1^R) = R(U = 0, t = \infty)$;
(iii) as the time $t_1^{\min}$ where the minimum of $R(t)/\rho(t)$ is reached (see Fig. 5);
(iv) as the time scale t_1^s allowing to map the curves $R(t)/\rho(t)$ onto a single scaling curve $R(t)/\rho(t) = f_s(t/t_1^s)$. The existence of such a scaling and the L_1 and U dependence of t_1^s are shown in Figure 8.

   We have checked that the definitions (iii) and (iv) are compatible. For $t < t_1$ the motion is essentially ballistic, and we expect that $t_1(L_1) \propto L_1$, as for a *clean* system of size $L = L_1$ (definition (i)) where a term of order $\pm U/L_1^2$
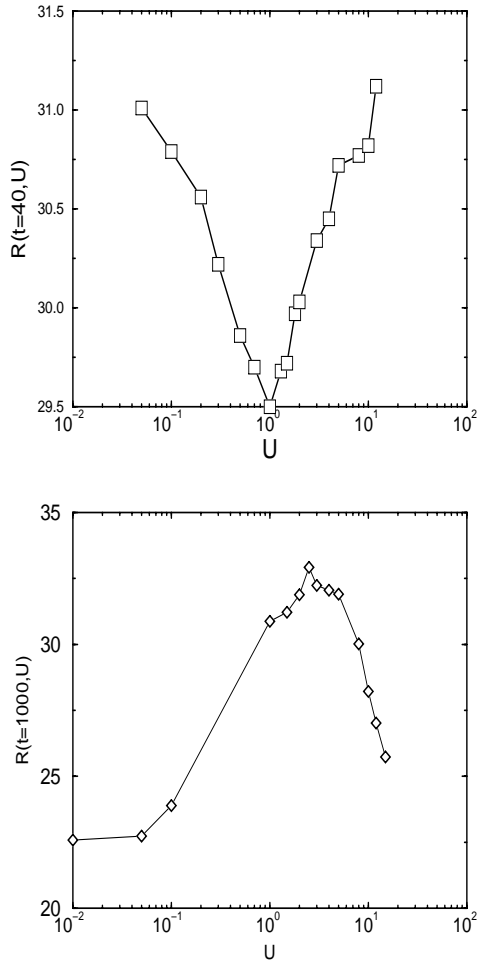
Fig. 7. Duality and inversion of the role of U: $R(t)$ averaged over 100 samples. Up: ballistic regime $t = 40 < t_1$, $L = L_1 = 200$. Down: sub-diffusive regime, $t = 1000$, $L = 512$, $L_1 = 36$.

coupled $\nu_1 \propto L_1$ free boson states.

$$\frac{t_1}{L_1} = f(U) \approx 1 - 0.3U.$$

The interesting feature of $t_1^{\min}$ is that $R \approx \rho$ at this time, as when $U = 0$. This time where there is an inversion of the effect of the interaction should be related to the size L where the TIP level curvature [3] does not depend on U. According to reference [3], this size is of order (but not exactly) L_1.

7 Very slow delocalization and weak critical chaos

After the ballistic propagation for $t < t_1$, the spreading of the center of mass measured by $R(t)$ saturates without interaction. This is due to one particle quantum interferences yielding one particle Anderson localization. When $U \neq 0$, this saturation is suppressed, but the spreading
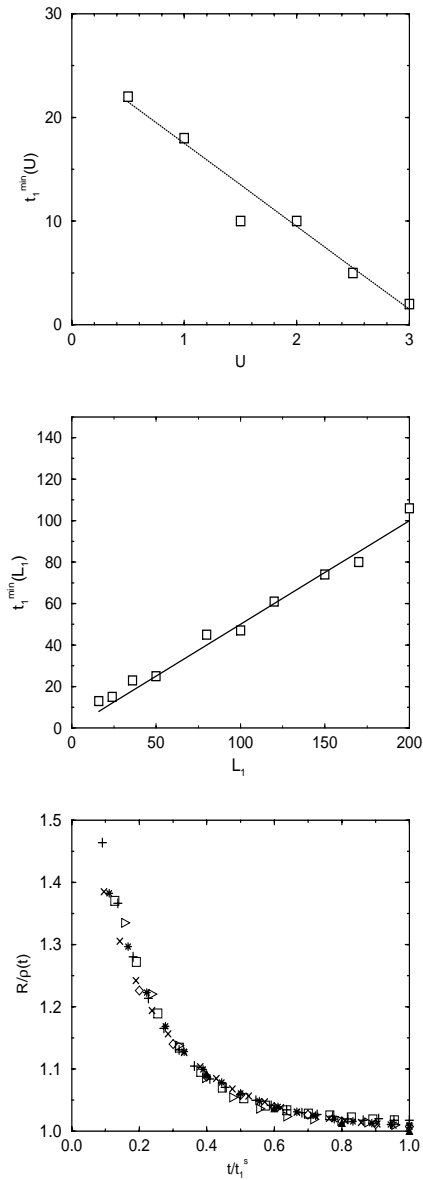

Fig. 8. Up: $t_1^{\min}(U)$ with $L_1 = 24$, $L = 256$ and 200 samples. The line is a linear fit: $t_1 = L_1 - 8U$. Middle: $t_1^{\min}(L_1)$ with $L \approx 3L_1$, $U = 1$ and 50 samples. The line is a linear fit: $t_1^{\min} = 0.5L_1$. Down: rescaling $R(t/t_1^s)$ with $L_1 = 24$, $U = 0.5$ (pluses), $U = 1$ (squares), $U = 1.5$ (diamonds), $U = 2$ (full triangles) and $U = 1$ $L_1 = 16$ (triangles), $L_1 = 36$ (stars), $L_1 = 50$ (crosses).

$R(t)$ has now a so slow increase that a logarithmic scale for the time t is appropriate.

Let us first consider the increase of the relative separation $\rho(t)$ between the two particles when interaction assisted propagation begins. As recalled in the Section 3.1, we expect a behavior given by

$$\rho(t) \approx L_1(1 + \ln(\Gamma_1 t)),$$

which turns out to be in good agreement with the numerical results. Plotting $\rho(x) - \rho(t_1)$ as a function of
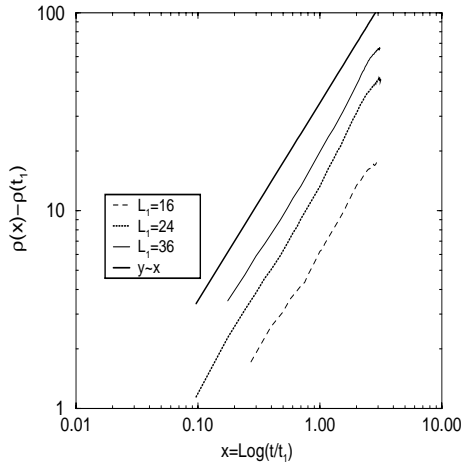
Fig. 9. Dynamics of the size of the pair: $\rho(x) - \rho(t_1)$ as a function of $x = \log(t/t_1)$ in log-log coordinates for $L_1 = 16, 24, 39$, $L = 512$ and $U = 1$.

Fig. 10. Slow delocalization of $R(t)$: $L_1 = 16$, $L = 1024$ and $U = 1$.

$x = \log(t/t_1)$, one can check in Figure 9 the predicted logarithmic behavior.

The evolution of the center of mass is on the contrary not described by the (modified) diffusion law

$$R(t) \approx \sqrt{D_2(t)t},$$

but has a much slower motion. However, this slow interaction induced delocalization is not very surprising since: (i) the hopping terms induced by the interaction between the free boson states (or the hard core boson states) are much smaller in one dimension than assumed in the random matrix model used to derive the non linear σ model of reference [8] (Sect. 3.1). The interaction matrix is not Gaussian and the effective density of coupled free boson states is significantly reduced (Sect. 3.3). Due to this multifractal perturbation, the lifetime of the free boson states is much larger than for a more normal (Gaussian) interaction matrix, as checked in reference [1].

(ii) For $L \approx L_1$, the interaction can only drive weak critical chaos (Sect. 3.4). For $L \geq L_1$, the spectrum becomes less rigid, with statistics intermediate between critical statistics and Poisson statistics. Indeed, for $L \geq L_1$, the TIP spectrum becomes a superposition of many states not reorganized by U and having uncorrelated fluctuations (Poisson) and a small part of states having critical statistics (weak critical chaos). With the chosen initial condition (two particles put close the one to the other at $t = 0$) one can argue that we mainly probe the few states with critical spectral statistics. Those critical statistics are associated with slow anomalous diffusion. Let us take one of those billiards with critical statistics: a right triangle [4] with smallest angle equal to $\pi/5$ and Dirichlet boundary conditions. For a very long time, the classical trajectories are stable, the system remains on the same KAM torus in phase space, until the corner with angle $4\pi/5$ is reached. At this moment only, the trajectories can escape from the original KAM torus and start to explore other part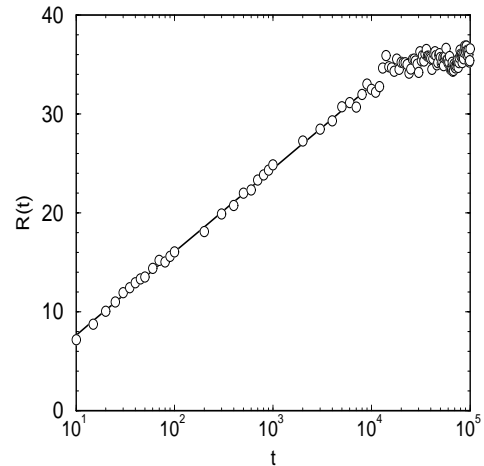s of the phase space. This suggests us a possible analogy between a single particle in the triangle billiard and the two particles in a disordered chain of size $\approx L_1$ with *on site interaction*: each particle is trapped in the one particle phase space between the collisions. Only after a collision, the frequency of those collisions being very low and depending on the strength of the random potential, the two particle phase space starts to be explored. This may explain the similarity with a single particle in the triangle. Critical statistics are associated with very slow explorations of the phase space, and hence of the real space. The fact that the interaction can never drive full quantum chaos, but only weak critical chaos, makes likely a very slow interaction assisted propagation. If the motion was isotropic in the plane (n_1, n_2), we should expect anomalous diffusion $(R^2(t) \approx t^\alpha)$ with $\alpha < 1$, as observed for a single particle at the mobility edge in three dimensions, where the spectral statistics are critical.

Since the motion is anisotropic in the plane (n_1, n_2), we do not find simple anomalous diffusion, but a simple $\log(t)$ behavior:

$$R(t) \propto \log(t), \tag{7}$$

as shown in Figure 10 for $L_1 = 16$ (see also Fig. 3 for $L_1 = 36$).

This logarithmic delocalization is not easy to explain, but reminds us the classical problem of a random walk in a percolating network. Without anisotropy, one gets anomalous diffusion. When one introduces anisotropy in the walk, it has been observed [13] that the dynamics is no longer described by a power law $R(t) \approx t^\alpha$, but by a $\log(t)$ law. If we order the localized one particle states $|\alpha\rangle$ by the location n_α of the center of their localization domain, from one side of the chain to the other, the TIP model in the free boson basis $|\alpha\beta\rangle$ is both anisotropic (larger hopping along the center of mass direction than along the other direction) and the hopping terms $\langle\alpha\beta|H_{\text{int}}|\gamma\delta\rangle$ have a multifractal measure. One can then argue that the two problems might be related, sharing the same $\log(t)$ spreading of $R(t)$.

8 Conclusion

In summary, this study of the TIP quantum motion has given some new insights on several aspects of the model. There are two length scales L_1 and L_2, and two corresponding time scales t_1 and t_2. For $L < L_1$ ($t < t_1$) the interaction defavors the pair propagation and reduces the level curvature. On the other hand, for $L > L_1$ ($t > t_1$), there is a very slow interaction assisted pair propagation and the level curvature increases as a function of U. Our main result is that this delocalization is very slow, in qualitative agreement with the concepts of interaction induced weak critical chaos and of multifractal hopping terms. Moreover, the wavefunction $|\Psi_{n_1,n_2}(t)|$ itself has multifractal features visible in Figure 1. With appropriate initial conditions, one can observe the symmetry $U \leftrightarrow A/U$. In conclusion, we underline that our results characterize symmetric states with purely on site interaction in strictly one dimension. It will be interesting to study if they remain valid for longer range interactions, or in a quasi-one dimensional limit, or if the behavior predicted from the σ model approach of reference [8] becomes valid.

References

1. X. Waintal, J.-L. Pichard, TIP I, Eur. Phys. J. B **6**, 117 (1998).
2. X. Waintal, D. Weinmann, J.-L. Pichard, TIP II, Eur. Phys. J. B **7**, 451 (1999).
3. A. Wobst, D. Weinmann, TIP IV, Eur. Phys. J. B **10**, 159 (1999).
4. E. Bogomolny, U. Gerland, C. Schmit, Phys. Rev. E **59**, R1315 (1998).
5. B.I. Shklovskii, B. Shapiro, B.R. Sears, P. Lambrianides, H.B. Shore, Phys. Rev. B **47**, 11487 (1993).
6. S. De Toro Arias, C. Vanneste, J. Phys. I France **7**, 1071 (1997).
7. D.L. Shepelyansky, Phys. Rev. Lett. **73**, 2067 (1994).
8. K. Frahm, A. Müller-Groeling, J-L. Pichard, Phys. Rev. Lett. **76**, 1509 (1996); Z. Phys. B **102**, 261 (1997).
9. E. Akkermans, J.-L. Pichard, Eur. Phys. J. B **1**, 223 (1998).
10. Y. Imry, Europhys. Lett. **30**, 405 (1995).
11. I.V. Ponomarev, P.G. Silvestrov, Phys. Rev. B **56**, 3742 (1997).
12. S. De Toro Arias, J.M. Luck, J. Phys. A: Math. Gen. **31**, 7699 (1998).
13. J. Dräger (private communication).